Dual-Functional Energy-Harvesting and Vibration Control: Electromagnetic Resonant Shunt Series Tuned Mass Dampers

Lei Zuo
e-mail: lei.zuo@stonybrook.edu

Wen Cui

Department of Mechanical Engineering,
State University of New York at Stony Brook,
Stony Brook, NY 11794

This paper proposes a novel retrofittable approach for dual-functional energy-harvesting and robust vibration control by integrating the tuned mass damper (TMD) and electromagnetic shunted resonant damping. The viscous dissipative element between the TMD and primary system is replaced by an electromagnetic transducer shunted with a resonant RLC circuit. An efficient gradient based numeric method is presented for the parameter optimization in the control framework for vibration suppression and energy harvesting. A case study is performed based on the Taipei 101 TMD. It is found that by tuning the TMD resonance and circuit resonance close to that of the primary structure, the electromagnetic resonant-shunt TMD achieves the enhanced effectiveness and robustness of double-mass series TMDs, without suffering from the significantly amplified motion stroke. It is also observed that the parameters and performances optimized for vibration suppression are close to those optimized for energy harvesting, and the performance is not sensitive to the resistance of the charging circuit or electrical load.
[DOI: 10.1115/1.4024095]

Keywords: energy harvesting, vibration control, multiple tuned mass dampers, electromagnetic shunt damping, resonant circuit

1 Introduction

Tall buildings, slender towers, and long bridges are subject to large vibration due to wind excitations, and tuned mass dampers (TMDs) have been widely used to suppress the vibration for human comfort and structure protection [1–3]. Recently the authors proposed to make dual use of the TMDs for both purposes of energy harvesting and vibration control [4] and experimentally demonstrated the feasibility by replacing the viscous damper with an electromagnetic transducer shunted with a resistive circuit [5]. Based on wind modeling and wind structure interaction, Ni et al. [6] showed that enhanced performance of vibration control and energy harvesting can be achieved by putting another reaction mass in series with the existing TMD; the total mass of a series of TMDs can be much smaller than the classic TMD to achieve the same effectiveness of vibration suppression but at the cost of several times of larger motion stroke of the electromagnetic harvester. In this paper, we propose a novel approach to attain the enhanced performance of dual-functional series TMDs without suffering from large motion stroke. This enables the retrofit implement of energy-harvesting series TMDs.

The key idea is to shunt the electromagnetic transducer between the TMD and the primary structure with a resonant *R-L-C* circuit, where *R* is the resistive load like the dc-dc charging circuit [7], *L* is the inductance of the electromagnetic transducer, and *C* is the capacitor of the shunt circuit. Such an idea is inspired by the shunting damping treatments in literature, initially used in piezoelectric structures and recently in electromagnetic devices. Forward [8] first demonstrated the passive circuit shunting for narrow-band reduction of resonant mechanical response in 1979. Hagood and von Flotow ([9]) analytically interpreted and experimentally proved that piezoelectric shunt with an *RL* circuit will act as a TMD. Extensive research has been done for shunted piezoelectric damping, as seen in the reviews [10,11] and references therein. Behrens et al. [12,13] presented the concept of electromagnetic resonant damping with an *RC* shunt circuit, and the tuning parameters were obtained numerically. Inoue et al. [14] obtained the analytical expressions of the optimal tuning frequency and damping, or the parameters of *L* and *R*, by following a similar approach of Den Hartog's fixed point method of TMD tuning [15]. Zhang et al. [16] proposed to use a negative inductor to cancel the inherent inductance of electromagnetic transducer and demonstrated that the first four vibration modes of a plate can be suppressed simultaneously as nonresistant viscous damping.

The main contribution of this paper is to demonstrate a series TMDs effect can be achieved by combining the mechanical resonance of a TMD and the electrical resonance of an RLC circuit for enhanced vibration damping or/and vibration energy harvesting. Another contribution of this paper is an efficient numeric method to minimize the vibration and maximize the electric power harvesting.

The paper is organized as following. Section 2 briefly introduces the dual-function TMD and electromagnetic TMD with highlight on the mechanical–electrical coupling and energy harvesting. Section 3 will present the electromagnetic resonant shunt series TMD and optimization methods based on system norm and matrix gradient in the decentralized control framework. The results of vibration suppression, energy harvesting, and parameter sensitivity based on the case study of Taipei 101 Tower are presented in Sec. 4, and conclusions follow in Sec. 5.

Contributed by the Design Engineering Division of ASME for publication in the Journal of Vibration and Acoustics. Manuscript received February 20, 2012; final manuscript received March 21, 2013; published online June 18, 2013. Assoc. Editor: Wei-Hsin Liao.

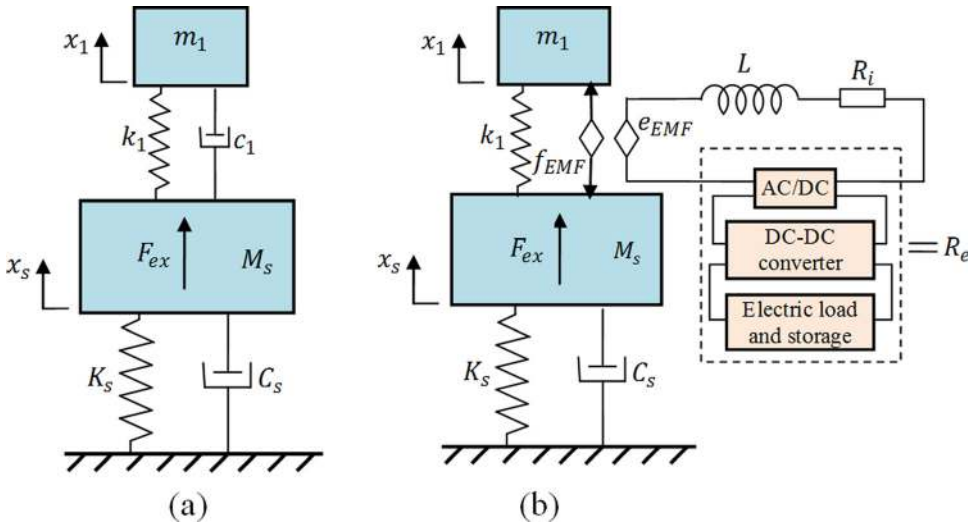

Fig. 1 (*a*) Classic TMD, (*b*) dual-functional TMD for energy harvesting and vibration control, where the damping c_1 is implemented with an electromagnetic transducer shunted with a resistive circuit

2 Electromagnetic TMDs and Dual-Functional TMDs

2.1 Energy-Harvesting TMD. Figure 1 shows the concept of a dual-functional TMD where the energy dissipative damping between the primary mass M_s and TMD mass m_1 is replaced with an electromagnetic transducer of coil resistance R_i and inductance L. The electromagnetic transducer can be either linear or rotational one with motion transmission. The relative motion between the TMD and primary system will produce a induced voltage e_{EMF} (traditionally called an "electromotive force" (EMF) responsible for flow of electrons in the circuit) proportional to the relative velocity

$$e_{\text{EMF}} = k_v(\dot{x}_1 - \dot{x}_s) \tag{1}$$

where k_v is the voltage constant of the electromagnetic transducer in V/(m/s). The electrical current in the electromagnetic transducer will produce a force f_{EMF} proportional to the electrical current $i = dq/dt$

$$f_{\text{EMF}} = k_f i = k_f \dot{q} \tag{2}$$

where k_f is the force constant in N/A. For an ideal transducer without energy loss, we have $k_v = k_f$.

If the electromagnetic transducer is shunted with the resistive load R_e (a dc–dc charging circuit can be modeled as a resistive load [5,7]), the electrical circuit equation will be

$$e_{\text{EMF}} + L\ddot{q} + R\dot{q} = 0 \tag{3}$$

where R is the total resistance of the circuit including the internal resistance of the transducer coil R_i and the external electric load resistance R_e: $R = R_i + R_e$.

When $j\omega L$ is much smaller than R, or L is cancelled by an external inductor in a way like that in Ref. [15], Eq. (3) becomes $e_{\text{EMF}} + R\dot{q} = 0$ and Eq. (1) will become

$$f_{\text{EMF}} = k_f i = -\frac{k_f k_v}{R}(\dot{x}_1 - \dot{x}_s) \tag{4}$$

which means that *the energy harvesting will also result in ideal viscous damping* with a coefficient as

$$c_1 = \frac{k_f k_v}{R} \tag{5}$$

Based on this principle, Tang and Zuo [5] implemented a dc–dc charging circuit to harvest energy while achieving the effect of classic TMD vibration control. The tuning rules of classic TMD can be used to choose c_1 and, thus, R (based on Eq. (5)), for example, using Den Hartog's rule [15]

$$f_{\text{opt}} = \frac{\omega_1}{\omega_s} = \frac{\sqrt{k_1/m_1}}{\omega_s} = \frac{1}{1+\mu}, \quad \xi_{\text{opt}} = \frac{c_1}{2m_1\omega_1} = \sqrt{\frac{3\mu}{8(1+\mu)}} \tag{6}$$

where μ is the mass ratio $\mu = m_1/M_s$. It should be noted that a type of regenerated control of active TMDs was demonstrated by the Yonemura et al. [17], in which an active control force is applied when the back electromotive voltage is less than the battery voltage (dead zone). Compared with Ref. [17], a dc–dc charging circuit has the advantage of minimizing the dead zone since the input voltage to the dc–dc booster charging circuit can be much smaller than the battery voltage.

2.2 Electromagnetic Shunt TMD. Figure 2 shows an electromagnetic resonant damping shunted with a capacitor C and a resistor $R = R_i + R_e$. The equation for this RLC circuit is

$$e_{\text{EMF}} + L\ddot{q} + R\dot{q} + \frac{1}{C}q = 0 \tag{7}$$

The resonant frequency of the circuit itself is

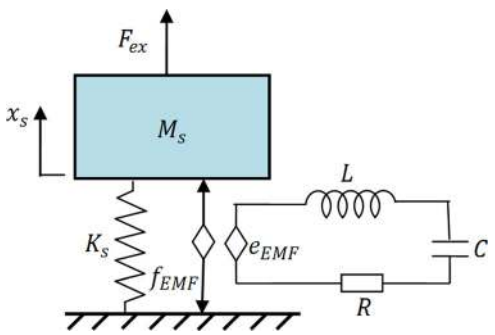

Fig. 2 A vibration system with electromagnetic resonant shunt circuit is similar as a TMD

$$\omega_e = 1/\sqrt{\mathrm{LC}} \tag{8}$$

And the electrical damping ratio of the circuit itself is

$$\xi_e = \frac{R}{2L\omega_e} \tag{9}$$

The relation of the external force F_{ex} and the displacement X_s can be obtained as

$$\left[M_s s^2 + K_s + \frac{k_f k_v s^2}{Ls^2 + Rs + \dfrac{1}{C}}\right] X_s = F_{\mathrm{ex}} \tag{10}$$

From Eq. (8) we see that if the whole electromagnetic transducer circuit has inductance only ($R=0$, $C=\infty$), $k_f k_v/L$ will act as an additional stiffness to K_s. Therefore,

$$\mu_k = \frac{k_f k_v}{LK_s} \tag{11}$$

This is called as *electromagnetic mechanical coupling coefficient*. It is actually a stiffness ratio (the electromagnetic mechanical coupling stiffness $k_f k_v/L$ divided by the stiffness K_s of the original system), which plays a similar role as the mass ratio in the classic TMD. Equation (8) also shows that if $R=0$ and $L=0$, $k_f k_v C$ will act as an additional mass. However, comparing with the X_s and F_{ex} relation of the classic TMD,

$$\left[M_s s^2 + K_s + \frac{m_1 s^2 (k_1 + c_1 s)}{m_1 s^2 + c_1 s + k_1}\right] X_s = F_{\mathrm{ex}} \tag{12}$$

one can that Eq. (8) is not exactly the same as the classic TMD, except for the undamped case $R=0$, where the single mass with LC shunted electromagnetic transducer is equivalent to an undamped absorber system.

An analytical expression obtained in Ref. [14] for such electromagnetic shunt TMD based on an electromagnetic mechanical coupling coefficient, or stiffness ratio μ_k (Eq. 9) using the fixed point method, which we simplify in Eq. (13). The frequency responses of electromagnetic shunt TMD are illustrated in Fig. 3 in comparison with that of the classic TMD.

$$f_{\mathrm{opt}} = \frac{\omega_e}{\omega_s} = \frac{\sqrt{1/\mathrm{LC}}}{\omega_s} = \sqrt{1-\mu_k/2}, \quad \xi_{\mathrm{opt}} = \frac{R}{2L\omega_e} \approx \frac{1}{2}\sqrt{\frac{3\mu_k}{2-\mu_k}} \tag{13}$$

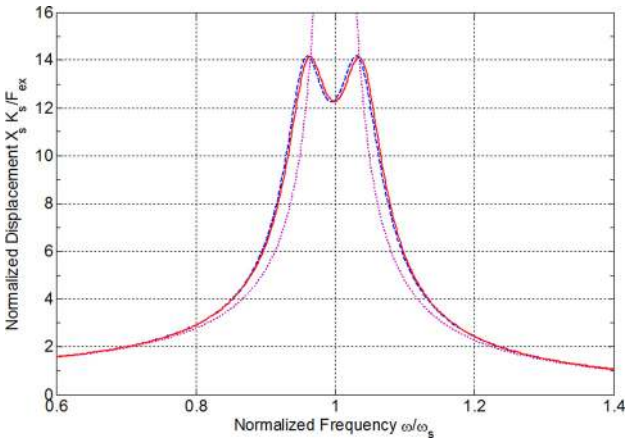

Fig. 3 The frequency responses of the classic TMD of mass ratio 1% with Den Hartog's tuning (dash) and electromagnetic shunt TMD of stiffness ratio 1% withtuning (solid) of Inoue et al. [14] compared with that of the primary without TMD (dot)

3 Electromagnetic Shunt Series TMDs, and Optimization for Vibration Control and Energy Harvesting

3.1 Concept of Electromagnetic Shunt Series TMD. Zuo [18] proposed the concept of series TMD and reported the enhanced effectiveness and robustness. Later Tao et al. [6] examined the application of series TMD for vibration control and energy harvesting of wind-induced tall building vibration. They concluded that two masses with 1.62% total mass ratio can attain the vibration control effect of the classic TMD of 2% mass, while harvesting a similar amount of energy. However, the motion stroke is six times larger, as shown in Fig. 4.

Instead of adding a second mass m_2, Fig. 5 shows our proposed new type of series TMD that is composed of an electromagnetic transducer, resonant shunt circuit, and the classic TMD. This configuration is similar to the energy-harvesting TMD in Fig. 1(*b*), however, with the significant difference that the electromagnetic transducer is shunted with an RLC circuit instead of a resistive circuit. The physical insight is that the "motion" is amplified in series, first by the TMD mechanical system then by the RLC electrical resonator.

The question is whether we can achieve the effect of a series TMD, and how to tune the parameters of stiffness k_1, capacitor C,

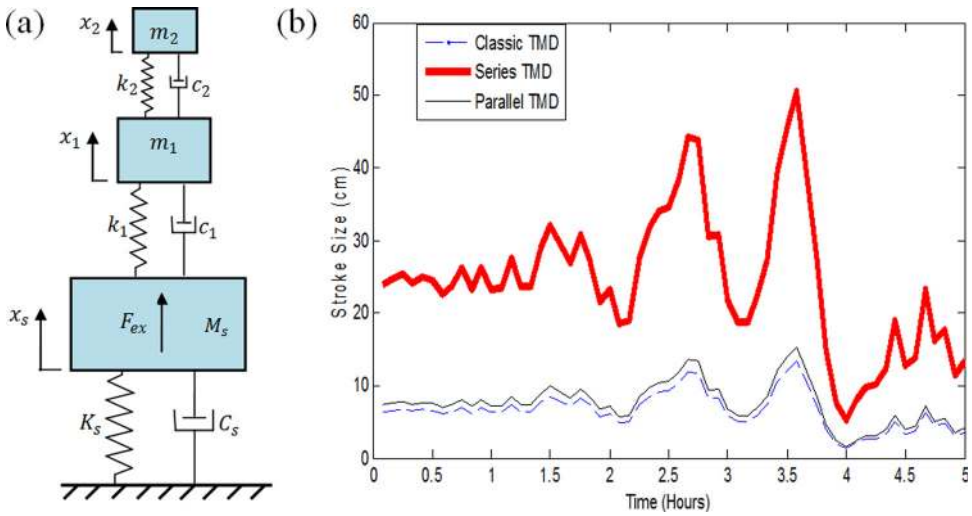

Fig. 4 (*a*) Double-mass series TMD, (*b*) the RMS stroke the double-mass series TMD is several times larger than the classic TMD or parallel TMDs [6]

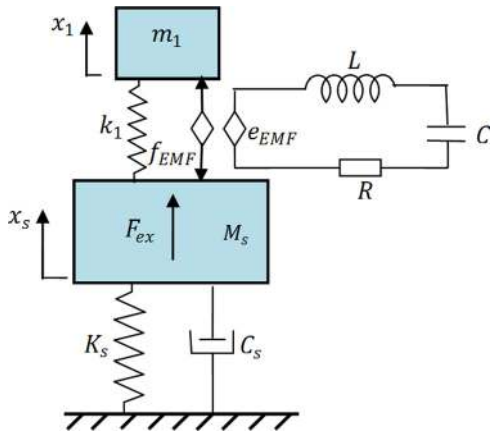

Fig. 5 The proposed series TMD with electromagnetic resonant shunt

and resistor R for a given electromagnetic transducer of inductance L, force constant k_f, and voltage constant k_v. Or equivalently, how to choose the dimensionless parameters:

- mechanical tuning ratio $f_1 = \omega_1/\omega_s = \sqrt{k_1/m_1}/\omega_s$
- electric tuning ratio $f_e = \omega_e/\omega_s = \sqrt{1/\mathrm{LC}}/\omega_s$ and
- electric damping ratio $\xi_e = R/2L\omega_e$

based on a given *electromagnetic mechanical coupling stiffness* $k_f k_v/L$ or *electromagnetic mechanical coupling coefficient* $\mu_k = k_f k_v/Lk_1$.

3.2 Parameter Optimization and Decentralized Control. To optimize the tuning parameters, we reformulate the problem of parameter optimization as a control problem by following the procedure proposed in Ref. [18]. As seen in Fig. 6, we replace the force of the spring k_1 as "control input" u_1:

$$u_1 = k_1(x_1 - x_s) \tag{14}$$

and the voltage on the resistor and capacitor as control input u_2:

$$u_1 = \frac{1}{C}q + R\dot{q} \tag{15}$$

And we take the "disturbance input" as $w = F_{\mathrm{ex}}$. The dynamics of the system can be written in the second order form

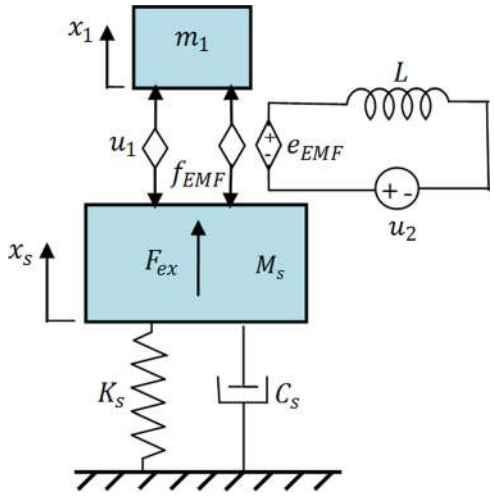

Fig. 6 The modeling of electromagnetic shunt series TMD as a control problem, where the control force u_1 is generated by the spring k_1, and the control force u_2 is produced by the electrical capacitor C and the resistor R

$$\begin{bmatrix} M_s & 0 & 0 \\ 0 & m_1 & 0 \\ 0 & 0 & L \end{bmatrix} \begin{pmatrix} \ddot{x}_s \\ \ddot{x}_1 \\ \ddot{q} \end{pmatrix} + \begin{bmatrix} C_s & 0 & k_f \\ 0 & 0 & -k_f \\ -k_v & k_v & 0 \end{bmatrix} \begin{pmatrix} \dot{x}_s \\ \dot{x}_1 \\ \dot{q} \end{pmatrix} + \begin{bmatrix} K_s & 0 & 0 \\ 0 & 0 & 0 \\ 0 & 0 & 0 \end{bmatrix} \begin{pmatrix} x_s \\ x_1 \\ q \end{pmatrix} = \begin{bmatrix} 1 \\ 0 \\ 0 \end{bmatrix} w + \begin{bmatrix} 1 & 0 \\ -1 & 0 \\ 0 & -1 \end{bmatrix} \begin{pmatrix} u_1 \\ u_2 \end{pmatrix} \tag{16}$$

By taking the state space variable as $x = (x_s, x_1, q, \dot{x}_s, \dot{x}_1, \dot{q})'$, the system can be written in state space form

$$\begin{aligned} \dot{x} &= Ax + B_{11}w + B_{12}u \\ z &= C_1x + D_{11}w + D_{12}u \\ y &= C_2x + D_{21}w + D_{22}u \end{aligned} \tag{17}$$

where z is the "performance output," such as the vibration of the primary system x_s or the electric current $\dot{q}$ in the circuit. And y is the "measurement output," $y = (x_1 - x_s, q, \dot{q})'$, used to generate control input u

$$u = \begin{pmatrix} u_1 \\ u_2 \end{pmatrix} = \begin{bmatrix} k_1 & 0 & 0 \\ 0 & 1/C & R \end{bmatrix} y = F_d y \tag{18}$$

Thus, the parameter optimization problem becomes a zero-order decentralized control problem (Fig. 7); once the block-diagonal feedback matrix F_d (Eq. (18)) is obtained, we can obtain the tuning parameters k_1, C, and R.

3.3 Optimization for Vibration Control and Energy Harvesting. Since the wind excitation force to civil structures is of broad bandwidth, in the following we will utilize H_2 control method, which has the physical meaning of *minimizing the root mean square (RMS) of z under unit white noise input w* [19]. White noise means the expectations $E[w(t)] = 0$ and $E[w(t-\tau)w(t)'] = \delta(\tau)I$, where $\delta(\tau)$ is a Dirac function. If the input w is harmonic excitation with unknown frequency, H_∞ control method can be used, which *minimizes the maximum peak in the frequency domain* [19].

The nice feature of decentralized H_2 control method is that the system H_2 norm (RMS of z under unit white noise input w) and its gradient $\partial \parallel H_{w\to z} \parallel_2^2 / \partial F_d$ (H_2 norm square with respect to the block-diagonal feedback matrix F_d) can be obtained analytically using matrix calculus, as derived by the author in Ref. [18].

$$\parallel H_{w\to z} \parallel_2^2 = \mathrm{trace}[(B_1 + B_2F_dD_{21})'K] \tag{19}$$

where matrix $\boldsymbol{K}$ (symmetric) is observability Grammian satisfying the Lyapunov equation

$$\begin{aligned} &K(A + B_2F_dC_2) + (A + B_2F_dC_2)'K \\ &\quad + (C_1 + D_{12}F_dC_2)'(C_1 + D_{12}F_dC_2) = 0 \end{aligned} \tag{20}$$

By employing the Lagrange multiplier method and matrix calculus, the closed form of the gradient $\partial \parallel H_{w\to z} \parallel_2^2 / \partial F_d$ can be obtained [18,20], as detailed in the Appendix.

Therefore, we can use gradient based optimization, such as Broyden–Fletcher–Goldfarb–Shanno (BFGS) quasi-Newton method [21], to find the matrix F_d that minimizes the system H_2 norm $\parallel H_{w\to z} \parallel_2$. It should be pointed out that, unlike the standard H_2 or linear-quadratic-Gaussian (LQG) control, "control force" u does not need to be a weighted part of cost output z to avoid a singularity problem since we do not use the *Riccati equation*.

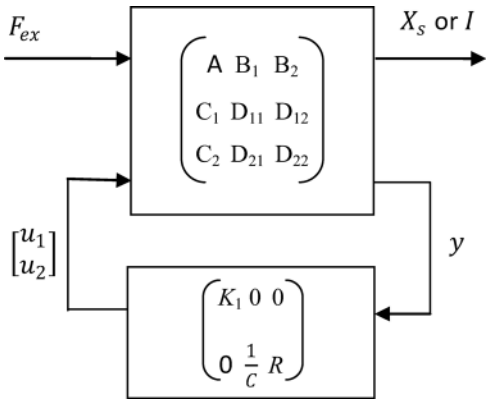

Fig. 7 The parameter optimization of the mechanical and electrical components in the framework of decentralized control

For vibration suppression, we choose the performance measurement z as the displacement, velocity, or acceleration of the primary system. The optimization procedure is similar to that in Ref. [18], which we omit here.

However, an unanswered question is whether the parameters optimized for vibration suppression are also the ones to maximize the energy harvesting. For energy harvesting, we would like to *maximize the average electrical power* on the resistive load R. Since the instant power is

$$P(t) = R\dot{q}(t)^2 \tag{21}$$

One may realize that the problem of maximizing the energy is not easy because the power $P(t)$ involves one state variable $\dot{q}(t)$ and one variable R in the feedback gain matrix F_d ($R = F_d$ (2,3)), and the problem is *maximization* instead of minimization in the standard H_2 control.

To solve the problem of maximizing the energy, we rewrite the objective function as the average power, which is proportional to the resistive load R and the RMS value of the current $\dot{q}(t)$, the latter of which can be calculated as the H_2 norm of system $H_{w\to\dot{q}}$

$$P_{\text{ave}} = R(\dot{q}_{\text{RMS}})^2 = R \parallel H_{w\to\dot{q}} \parallel_2^2 \tag{22}$$

Hence, two factors can be observed: (1) The objective function P_{ave} can be evaluated for a given feedback matrix F_d (composed of k_1, C, and R) by calculating the system H_2 norm from w to the electrical current $\dot{q}$, $\parallel H_{w\to\dot{q}} \parallel_2$, using Eq. (19); (2) The gradient of average power P_{ave} with respect to the block-diagonal feedback gain matrix F_d can be evaluated using the chain rule

$$\frac{dP_{\text{ave}}}{dF_d} = R\frac{\partial \parallel H_{w\to z} \parallel_2^2}{\partial F_d} + \frac{\partial R}{\partial F_d} \parallel H_{w\to z} \parallel_2^2 \tag{23}$$

where the matrix gradient $\partial \parallel H_{w\to z} \parallel_2^2 / \partial F_d$ can be obtained using Eq. (A2) in the Appendix, and matrix gradient $\partial R/\partial F_d$ can be obtained from Eq. (18) as

$$\frac{\partial R}{\partial F_d} = \begin{bmatrix} 0 & 0 & 0 \\ 0 & 0 & 1 \end{bmatrix}$$

Therefore, we can use the gradient based optimization methods [21] to obtain the block-diagonal feedback matrix F_d that maximizes the electrical power harvested. Please note the system stability can be ensured if we replace F_d as

$$\begin{bmatrix} \bar{k}_1^2 & 0 & 0 \\ 0 & \frac{1}{\bar{C}^2} & \bar{R}^2 \end{bmatrix}$$

and the gradient can be modified correspondingly.

4 Case Study Based on Taipei 101 Tower

In this section we take the Taipei 101 tower as a case study and illustrate the electromagnetic shunt series TMD for energy harvesting and vibration control. Results are presented in comparison with the dual-functional TMDs with classic one mass and two masses in series.

Taipei 101 is one of the tallest building in the world (449.2 m to roof, and 509.2 m to spire). A TMD of 660 metric tonnes (728 short tons) is suspended on the top of the building from the 92nd to the 87th floor to suppress the wind induced vibration. Up to 40 KW of energy dissipation (average 15–20 KW) is expected in a 100-year wind event from one of the eight viscous damping devices between the primary structure and TMD [22]. The TMD is 0.78% of the modal mass, the first natural frequency is 0.146 Hz, and inherent damping of the building is 1%. In the case study, the parameters of the classic TMD are designed using the H_2 optimization, and the parameter of series TMDs of total mass ratio 0.78% are obtained using the H_2 design chart in Ref. [18] with the optimal mass distribution $m_2/(m_1+m_2) = 1.56\%$, as shown in Table 1. For the dual-functional implementation without circuit resonance, the damping c_1 (Fig. 1(*a*)) or c_2 (Fig. 4) can be realized using an electromagnetic transducer shunted with a resistive electrical load (Figs. 1(*b*) and 5).

4.1 Results of Electromagnetic Shunt Series TMD for Vibration Suppression. We assume the eletromagnetic transducer has an inductance $L = 0.25$ Hs, force constant $k_f = 150$ N/A, and voltage constant $k_v = 150$ V/(m/s). The electromagnetic mechanical coupling stiffness $k_f k_v/L = 9000$ N/m. We keep the total mass of TMD as 6.60×10^5 kg.

The gradient based optimization based of the decentralized H_2 control framework will yield the following matrix to *minimize* the displacement x_s under random force input F_{ex}, $\parallel H_{w\to z} \parallel_2 = 3.707 \times 10^{-8}$ m

$$F_d = \begin{bmatrix} k_1 & 0 & 0 \\ 0 & \frac{1}{C} & R \end{bmatrix} = \begin{bmatrix} 5.4963 \times 10^5 & 0 & 0 \\ 0 & 0.20991 & 0.03532 \end{bmatrix}$$

which means

- $k_{1\text{-opt}} = 5.4963 \times 10^5$ N/m
- $C_{\text{opt}} = 4.763$ Farads
- $R_{\text{opt}} = 0.03532\ \Omega$

The optimal vibration performances, including the vibration amplitude of the building, stroke of the harvester and harvesting power, of the electromagnetic shunt series TMD are shown in Table 2. The normalized frequency response of the building displacement with electromagnetic shunt series TMD is shown in Fig. 8 in comparison with that of the classic TMD and double-mass series TMD.

Table 2 shows that the vibration control and energy harvesting performances of an electromagnetic shunt series TMD are very close to those of double-mass series TMD, as we expected. These

Table 1 Parameters of Taipei 101 Tower and the H_2 optimal classic and double-mass series TMDs

System	Mass (Kg)	Stiffness (N/m)	Damping (N s/m)
Building without TMD	$M_s = 8.46 \times 10^7$	$K_s = 7.12 \times 10^7$	$c_s = 1.55 \times 10^6$ ($\zeta_s = 1\%$)
Classic TMD $\mu = 0.78\%$	$M_s = 8.46 \times 10^7$ $m_1 = 6.60 \times 10^5$	$K_s = 7.12 \times 10^7$ $k_1 = 5.48 \times 10^5$	$c_s = 1.55 \times 10^6$ $c_1 = 5.30 \times 10^4$
Double-mass series TMDs $\mu = 0.78\%$	$M_s = 8.46 \times 10^7$ $m_1 = 6.495 \times 10^5$ $m_2 = 1.05 \times 10^4$	$K_s = 7.12 \times 10^7$ $k_1 = 5.55 \times 10^5$ $k_2 = 8.52 \times 10^3$	$c_s = 1.55 \times 10^6$ $c_1 = 0$ $c_2 = 1.388 \times 10^3$

Table 2 Performances of optimal electromagnetic shunt series TMD in comparison with classic and double-mass series TMDs for Taipei 101[a] under unit white-noise force excitation F_{ex}

System	Vibration $X_{s\text{-rms}}$ (m)	Stroke ΔX_{rms} (m)	Harvesting[a] $\sqrt{P_{ave}}$ ($\sqrt{W}$)	Dissipation[a] $\sqrt{c_s}\,\dot{x}_s\vert_{rms}$ ($\sqrt{W}$)
Without TMD	6.726×10^{-8}	—		7.688×10^{-5}
Classic TMD	3.892×10^{-8}	2.724×10^{-7}	6.272×10^{-5}	4.445×10^{-5}
Double-mass series TMDs	3.704×10^{-8}	1.721×10^{-6} $(\Delta x = x_1 - x_2)$	6.416×10^{-5}	4.234×10^{-5}
Electromagnetic shunt series TMD	3.707×10^{-8}	3.24×10^{-7} $(\Delta x = x_1 - x_s)$	6.417×10^{-5}	4.233×10^{-5}

[a]Note: Harvesting means the energy harvested by the electromagnetic transducer, and dissipation refers to the power dissipated by the inherent damping C_s of the primary system.

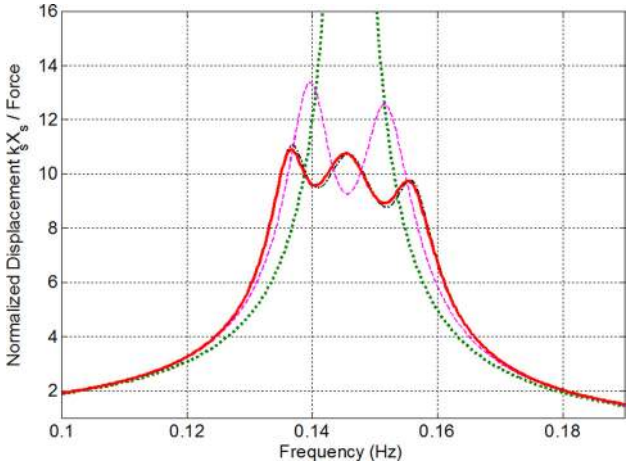

Fig. 8 The frequency responses of electromagnetic shunt series TMD for Taipei 101 Tower (solid) in comparison with double-mass TMD (dashed-dotted), classic TMD (dash), and system without TMD (dot), where all parameters are optimized to minimize the H_2 norm from external force to the displacement of the primary system

two types of series TMDs are better than the classic TMD. In terms of the stroke of the energy harvester (in the third column of Table 2), we see that the *stroke of the double-mass series TMD is 6.3 times as that of classic TMD, but the stroke of electromagnetic shunt series TMD is just increased by 19%*. Table 2 also indicates that *the harvestable energy from the TMD systems is 41–51% more than the energy dissipated by the primary damping*. It is also noted that the total energy taken out of the building using TMDs and primary damping is 39% more than the energy dissipated only by primary damping in building without TMDs.

Note that as long as the dimensionless parameters

- electromagnetic mechanical coupling coefficient $\mu_k = k_f k_v / L k_1$
- mechanical tuning ratio $f_1 = \omega_1/\omega_s = \sqrt{k_1/m_1}/\omega_s$
- electric tuning ratio $f_e = \omega_e/\omega_s = \sqrt{1/\mathrm{LC}}/\omega_s$
- electric damping ratio $\xi_e = R/2L\omega_e$

are the same, the overall system performance will be the same. This feature allows us to choose more practical parameters in the implementation. For the example, in this case study if $L = 0.25$ H is too large to implement, we can decrease k_f and k_v to half (which can be realized by reducing the motion transmission [4] or choosing smaller generator), and correspondingly decrease L and R to a quarter, and increase the C by four times.

4.2 Results of Electromagnetic Shunt Series TMD for Energy Harvesting. We also optimize the parameters of stiffness k_1 and the electrical capacitor C and resistor R to maximize the harvesting power using the gradient based method proposed in Sec. 3.3. The results are compared with the ones optimized for vibration control, as shown in Table 3. The frequency responses from excitation force F_{ex} to the building displacement x_s are shown in Fig. 9. We see that the parameters and performance are very close in these two cases, which means that the parameters for best energy harvesting can also achieve good vibration suppression.

The frequency responses from external force F_{ex} to the square root of harvesting power $\sqrt{P} = \sqrt{R}|\dot{q}|$ of electromagnetic shunt series TMDs are compared in Fig. 10 where the square root of the power of the classic TMD is $\sqrt{c_1}|\dot{x}_1 - \dot{x}_s|$ and that of double-mass series TMD is $\sqrt{c_1}|\dot{x}_2 - \dot{x}_1|$. Again we see the electromagnetic series TMDs perform similar as the double-mass series TMD. Both outperform the classic TMD in power harvested due to broader bandwidth effect, and for electromagnetic series TMDs we do not need to worry about the amplified stroke.

It is also interesting to note from the fourth and fifth columns of Table 2 that the energy extracted by the dual-functional TMDs is 50% more than that of the energy dissipation by the primary damping of the Taipei 101 building with TMDs.

4.3 Robustness of Vibration Suppression and Energy Harvesting to Tuning Parameters. In practice it is difficult to make perfect tuning for the parameters k_1, C, and R, or some parameter may change after a certain time. It is noted that the tolerance of the electrical components C and R is usually 1–5% or less.

Table 3 Optimal parameters and performances of electromagnetic shunt series TMDs optimized for vibration control and for energy harvesting under unit white-noise force excitation F_{ex}

Electromagnetic shunt series TMD system	Stiffness k_1 (N/m)	R and C (Ω or F)	Vibration $X_{s\text{-rms}}$ (m)	Stroke ΔX_{rms} (m)	Harvesting $\sqrt{P_{ave}}$ ($\sqrt{W}$)
Optimized for vibration control	5.496×10^5	0.353Ω 0.476F	3.704×10^{-8}	3.2426×10^{-7}	6.417×10^{-5}
Optimized for energy harvesting	5.540×10^5	0.351Ω 0.473F	3.707×10^{-8}	3.2431×10^{-7}	6.419×10^{-5}

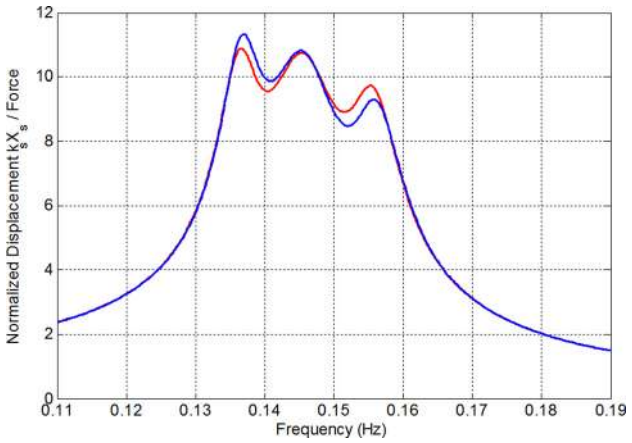

Fig. 9 The frequency response of the electromagnetic series TMD optimized for vibration suppression (solid) and optimized for energy harvesting (dash) for Taipei 101 Tower

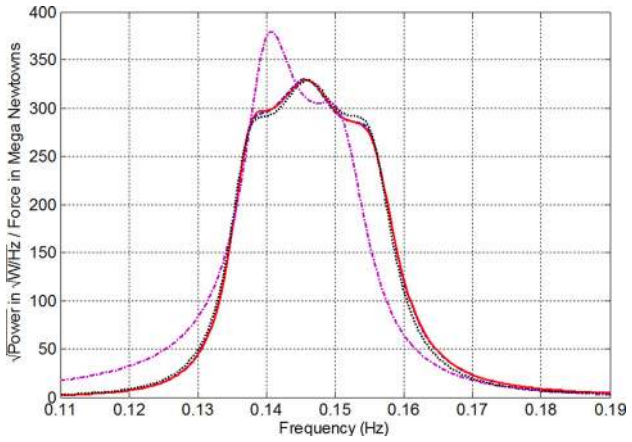

Fig. 10 The linear power spectrum density ($\sqrt{W/Hz}$) of harvested energy in electromagnetic series TMD system optimized for energy harvesting under white-noise force excitation (solid) and optimized for vibration suppression (dash) in comparison with the classic TMD (dashed-dotted) and double-mass series TMD (dot)

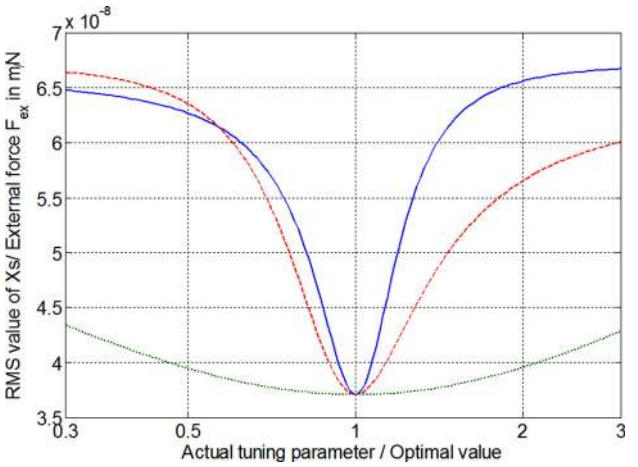

Fig. 11 The frequency responses of the electromagnetic series TMD (left) and the classic TMD (right) after 5% changes of the tuning parameters (k_1, C, R) or (k_1, c_1). The electromagnetic series TMD is more robust than the classic TMD.

To check the robustness, Fig. 11(*a*) shows the frequency responses of electromagnetic series TMD after 5% changes in the tuning parameters of k_1, C, and R. As a comparison, we also plot the frequency response of classic TMD under 5% changes in the tuning parameters of k_1, and c_1. We can see that the electromagnetic series TMD is much more robust than the classic TMD.

To further investigate the sensitivity of the performance of the tuning parameters k_1, C, and R, we plot the root mean square of the vibration amplitude and the square root of the harvested power under unit white-noise excitation force F_{ex} when the parameters change from 1/3 to three times of the optimal value, as shown in Figs. 12 and 13. We see that the performance is less sensitive to the change of electrical load R than the changes of capacity C and stiffness k_1. In energy harvesting, the value of electrical load R is an equivalent resistor of the charging circuit. The insensitivity to R gives us some convenience to control the charging circuit, for example, for voltage regulation.

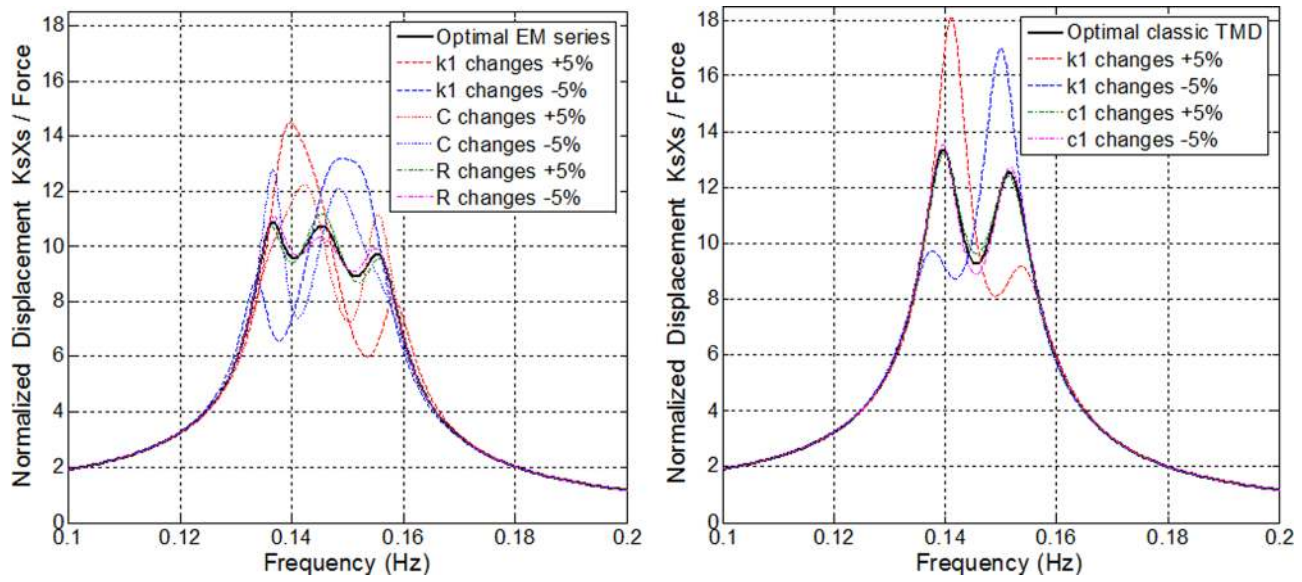

Fig. 12 Sensitivity of vibration suppression of the electromagnetic shunt series TMD for Taipei 101 to the changes of tuning parameters: stiffness k_1 (solid), capacitor C (dash), and electrical load R (dot) under unit white-noise force excitation F_{ex}

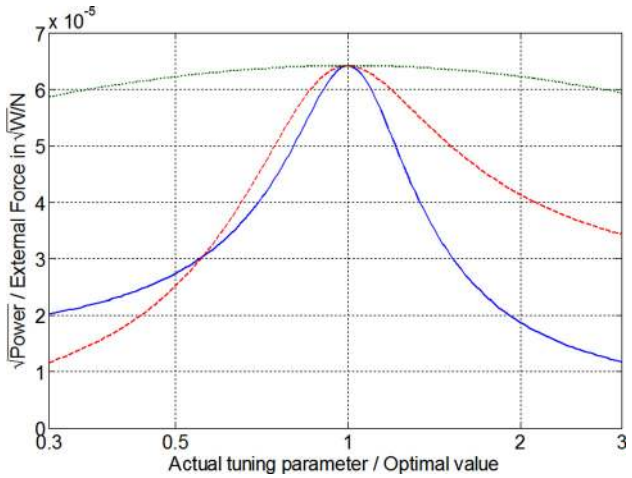

Fig. 13 Sensitivity of energy harvesting of the electromagnetic shunt series TMD for Taipei 101 to the changes of tuning parameters: stiffness k_1 (solid), capacitor C (dash), and electrical load R (dot)

Conclusions

This paper presents the electromagnetic shunt series TMD with application to simultaneous vibration control and energy harvesting. By tuning both the resonances of the TMD subsystem and the RLC charging circuit subsystem close to that of the primary structure, we achieve the enhanced performance of series TMD without suffering from large motion stroke as in the double-mass series TMD. Decentralized H_2 control and gradient based methods are used for the optimization of individual parameters. The performance is limited by the transducer's electromagnetic mechanical electromagnetic mechanical coupling coefficient $\mu_k = k_f k_v / L k_1$. The case study of Taipei 101 TMD system indicates that the electromagnetic shunt series TMD provides better vibration control and energy harvesting. And the motion stroke of the energy harvester only increases by 19% instead of 6.3 times in double-mass series TMD. The parameters optimized for best vibration suppression are very close to that optimized for best energy harvesting. Such a proposed approach with combined mechanical resonance and electrical resonance will greatly simplify and lead to practical and retrofitable implementation of series TMDs for energy harvesting and vibration suppression.

Acknowledgment

The author gratefully acknowledge the funding support from US National Science Foundation (NSF), CMMI#1031038.

Nomenclature

M_s, m_1, m_2 = masses of the primary system and tuned mass dampers
K_s, k_1, k_2 = stiffness of the primary system and tuned mass dampers
C_s, c_1, c_2 = damping of the primary system and tuned mass dampers
x_s, x_1, x_2 = displacement of the primary system and tuned mass dampers
R, R_i, R_e = resistances of generator coil, external load, and sum (Ω)
L = inductance of generator coil (H)
C = capacitance of the circuit (F)
k_f = back electromotive force (EMF) constant (N/A)
k_v = back electromotive voltage constant (V/(m/s))
f_{EMF} = back electromotive force (N)
e_{EMF} = back electromotive voltage (V)
μ_k = electromagnetic mechanical coupling coefficient
F_{ex} = external disturbance force (N)
q, i = charge (C) and current (A) of the electrical circuit
$\omega_s, \omega_1, \omega_e$ = natural frequencies of the primary, TMD, and electric circuit
f_{opt} = optimal frequency tuning of classic or electromagnetic TMD
ξ_{opt} = optimal damping ratio of classic or electromagnetic TMD
f_1 = mechanical frequency tuning ratio $f_1 = \omega_1/\omega_s$
f_e = electrical frequency tuning ratio $f_1 = \omega_1/\omega_s$
ξ_e = electrical damping ratio $f_1 = R/2L\omega_e$
$A, B_{11}, B_{12}, C_{11}, C_{12}, D_{11}, D_{12}, D_{21}, D_{22}$ = state space description matrices
x = state variable (vector) in state space
y,z = measurement and performance output in state space
w = disturbance input in state space
P, P_{ave} = power and average power (W)
F_d = decentralized feedback matrix
$H_{w\to z}$ = transfer function from w to z
$\| \|_2^2$ = system H_2 norm
$d/d, \partial/\partial$ = gradient and partial gradient

Appendix: Gradient of the System H_2 Norm to the Decentralized Feedback Matrix $\partial \|H_{w\to z}\|_2^2 / \partial F_d$

By introducing a symmetric Lagrange multiplier matrix $\boldsymbol{L}$ we can define Lagrange function from Eqs. (19) and (20) as

$$\begin{aligned}\mathcal{L}(F_d, K, L) = \text{trace}[&(B_1 + B_2 F_d D_{21})' K \\ &+ \text{trace}\{\left[K(A + B_2 F_d C_2) + (A + B_2 F_d C_2)' K\right. \\ &\left.+ (C_1 + D_{12} F_d C_2)'(C_1 + D_{12} F_d C_2)\right] L\}\end{aligned} \tag{A1}$$

Using matrix calculus, the *closed form* of the gradient $\partial \|H_{w\to z}\|_2^2 / \partial F_d$ can be obtained [18,20]

$$\begin{aligned}\frac{\partial \|H_{w\to z}\|_2^2}{\partial F_d} = 2[&(D_{12}' D_{12} F_d C_2 + D_{12}' C_1 + B_2' K) L C_2' \\ &+ B_2' K (B_1 + B_2 F_d D_{21}) D_{12}'] \odot F_p\end{aligned} \tag{A2}$$

where we use entry-by-entry multiplication $\odot$ to pick out the entries corresponding to the design variables $(k_1, 1/C, R)$ in F_d, and

$$F_p = \begin{bmatrix} 1 & 0 & 0 \\ 0 & 1 & 1 \end{bmatrix}$$

The Lagrange multiplier matrix $\boldsymbol{L}$ can be obtained by solving the Lyapunov equation for a given F_d

$$\begin{aligned}&L(A + B_2 F_d C_2)' + (A + B_2 F_d C_2) L \\ &+ (B_1 + B_2 F_d D_{21})(B_1 + B_2 F_d D_{21})' = 0\end{aligned} \tag{A3}$$

And the observability Grammian matrix $\boldsymbol{K}$ can be obtained by solving the Lyapunov equation Eq. (20) for a given F_d. It is noted that Lyapunov equations are linear and can be easily solved using standard codes the Matlab function lyap.

References

[1] Kareem, A., Kijewski, T., and Tamura, Y., 1999, "Mitigation of Motions of Tall Buildings With Specific Examples of Recent Applications," Wind Struct., **2**(3), pp. 201–251.

[2] Lackner, M. A., and Rotea, M. A., 2011, "Passive Structural Control of Offshore Wind Turbines," Wind Energ., **14**(3), pp. 373–388.
[3] Miyata, T., 2003, "Historical View of Long-Span Bridge Aerodynamics," J. Wind Eng. Ind. Aerodyn., **91**, pp. 1393–1410.
[4] Tang, X., and Zuo, L., 2010, "Regenerative Semi-Active Control of Tall Building Vibration With Series TMDs," Proceeding of America Control Conference, Baltimore, MD, June 30–July 2.
[5] Tang, X., and Zuo, L., 2012, "Simulation and Experiment Validation of Simultaneous Vibration Control and Energy Harvesting From Buildings Via Tuned Mass Dampers," Proceeding of America Control Conference, San Francisco, CA, June 29–July 1.
[6] Ni, T., Zuo, L., and Kareem, A., 2011, "Assessment of Energy Potential and Vibration Mitigation of Regenerative Tuned Mass Dampers on Wind Excited Tall Buildings," 2011 ASME Design Engineering Technical Conferences, Washington DC, August 28–31.
[7] Lefeuvre, E., Audigier, D., Richard, C., and Guyomar, D., 2007, "Buck-Boost Converter for Sensorless Power Optimization of Piezoelectric Energy Harvester," IEEE T. Power Electron., **22**(5), pp. 2018–2025.
[8] Forward, R. L., 1979, "Electronic Damping of Vibrations in Optical Structures," Appl. Opt., **18**, pp. 690–69.
[9] Hagood, N. W. and von Flotow, A., 1991, "Damping of Structural Vibrations With Piezoelectric Materials and Passive Electrical Networks," J. Sound Vib., **146**(2), pp. 243–268.
[10] Moheimani, S. O. R., 2003, "A Survey of Recent Innovations in Vibration Damping and Control Using Shunted Piezoelectric Transducers," IEEE Trans. Contr. Sys. Tech., **11**(4), pp. 482–494.
[11] Lesieutre, G. A., 1998, "Vibration Damping and Control Using Shunted Piezoelectric Materials," Shock Vib. Dig., **30**(3), pp. 187–195.
[12] Behrens, S., Fleming, A. J., and Moheimani, S., 2003, "Electromagnetic Shunt Damping," Proceedings of the IEEE/ASME International Conference on Advanced Intelligent Mechatronics (AIM 2003), Kobe, Japan, July 20–24, pp. 1145–1150.
[13] Behrens, S., Fleming, A. J., and Moheimani, S., 2005, "Passive Vibration Control Via Electromagnetic Shunt Damping," IEEE/ASME Trans. Mechatron., **10**(1), pp. 118–122.
[14] Inoue, T., Ishida, Y., and Sumi, M., 2008, "Vibration Suppression Using Electromagnetic Resonant Shunt Damper," ASME J. Vib. Acoust., **130**(4), p. 041003.
[15] Den Hartog, J. P., 1947, *Mechanical Vibration*, McGraw-Hill, New York.
[16] Zhang, X., Niu, H., and Yan, B., 2012, "A Novel Multimode Negative Inductance Negative Resistance Shunted Electromagnetic Damping and Its Application on a Cantilever Plate," J. Sound Vib., **331**(10), pp. 2257–2271.
[17] Yonemura, J., Kim, S., Mikami, H., Nagai, B., and Okada, Y., 1999, "Regenerative Control of Active Mass Type Vibration Damper," Trans. Jap. Soc. Mech. Eng. C., **65**(632), pp. 1374–1380 (in Japanese).
[18] Zuo, L., 2009, "Effective and Robust Vibration Control Using Series Multiple Tuned Mass Dampers," ASME J. Vib. Acoust., **131**(3), p. 031003.
[19] Zhou, K., Doyle, J. C., and Glover, K., 1995, *Robust and Optimal Control*, Prentice-Hall, Englewood Cliffs, NJ.
[20] Zuo, L., and Nayfeh, S., 2005, "Optimization of the Individual Stiffness and Damping Parameters in Multiple-Tuned-Mass-Damper Systems," ASME J. Vib. Acoust., **127**(1), pp. 77–83.
[21] Bertsekas, D. P., 1995, *Nonlinear Programming*, Athena Scientific, Belmont, MA.
[22] Haskett, T., Breukelman, B., Robinson, J., and Kottelenberg, J., 2004, "Tuned-Mass Damper Under Excessive Structural Excitation," Report of the Motioneering Inc., Guelph, Ontario, Canada.